Spring 2018

Observations of Ion Density and Temperature around the International Space Station During two Geomagnetic Storms

Alex M. Wright
University of New Hampshire, Durham, mtt3@wildcats.unh.edu

Observations of Ion Density and Temperature around the International Space Station During two Geomagnetic Storms

Alex Wright

Advisors: Jichun Zhang and Lynn Kistler

Department of Physics - University of New Hampshire

Undergraduate Thesis

April 29, 2018

Abstract

The International Space Station (ISS) is a low Earth orbit research facility and host to an international crew. Geomagnetic storms cause changes in the Earth's magnetic field and affect the ion density and temperature in the ionosphere which could pose a hazard to ISS crew. This hazard is measured by the Floating Potential Measurement Unit (FPMU) which measures ion density, ion temperature, and the charge differential of the ISS relative to its surrounding environment. I analyzed data collected by Narrow Sweep Langmuir Probe for two storms in 2015. Ion density and temperature were affected by geomagnetic storms, but the effects were less than those found due to normal orbital conditions.

Nomenclature

CDAweb – Coordinated Data Analysis Web
CME – Coronal Mass Ejection
Dst – Disturbance Storm Time Index
FPMU – Floating Potential Measurement Unit
FPP – Floating Potential Probe
IDL – Interactive Data Language
ISS – International Space Station
MLAT - Magnetic Latitude
MLT - Magnetic Local Time
NAN – Not A Number
NLP – Narrow Sweep Langmuir Probe
PIP – Plasma Impedance Probe
WLP – Wide Sweep Langmuir Probe

Introduction

In 2006 the Floating Potential Measurement Unit (FPMU) was installed on the International Space Station[1]. Its purpose was to identify potentially hazardous times for the crew to conduct extra vehicular activities. The unit is composed of four different probes that in combination make measurements of the electric potential of the space station relative to the surrounding environment, the ion density, and the ion temperature.

While its main purpose was to improve crew safety, the measurements of the FPMU can also be used to study the surrounding plasma and observe how different factors influence the surrounding space environment.

I analyzed data from two different geomagnetic storms: a moderate storm on 2015-09-20 and an intense storm on 2015-12-20. The data used came from the Narrow Sweep Langmuir Probe located on the FPMU. I found that while the storms did have an affect on the surrounding plasma, the effect was not as large as normal orbital effects had.

Background

International Space Station (ISS)

The ISS is a space environment research facility. The first module was launched in 1998 from Russia[2]. The first international crew began permanent residence in November of 2000. The station orbits in the F-layer of the ionosphere at about 400 km. Hundreds of experiments have been carried out aboard since its launch.

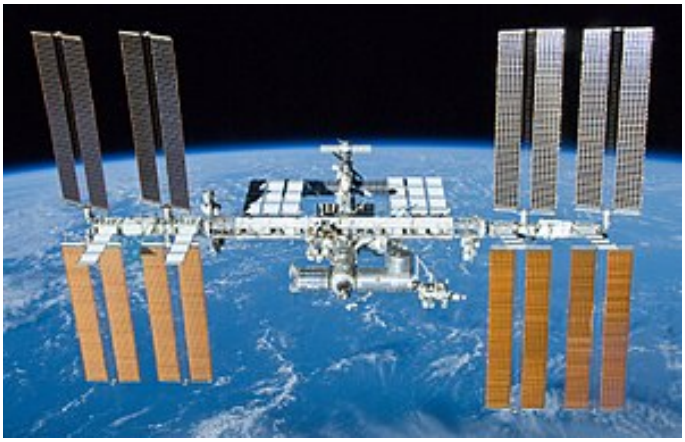

Figure 1 *- The International Space Station*

Floating Potential Measurement Unit (FPMU)

The FPMU is an instrument used to measure electric potential, ion density, and ion temperature. NASA identified unusual charging aboard the ISS due to the solar panels collecting electrons faster than they could be discharged, causing the ISS to develop a negative potential relative to the surrounding plasma (gas of ionized particles)[3].

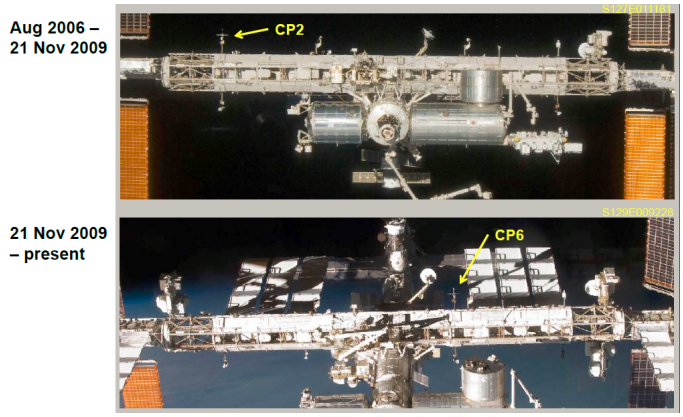

Figure 2 *- Locations of the FPMU*

The FPMU was made primarily to measure this potential. It was designed and built by Utah State University Space Dynamics Laboratory in 2003[4]. It was originally installed on the S1 truss of the ISS on August 3, 2006[5], shown in the top panel of Figure 2 by the yellow arrow. On November 21, 2009 it was moved[6], shown in the bottom panel of Figure 2. By identifying unusual charging events and hazardous periods it improved the safety of the crew by alerting them when Extra Vehicular Activity should not be performed. In addition the unusual charging events could identify arcing along the surface of the ISS which could lead to surface degradation or electronic anomalies in some areas[7]. However the FPMU is not always on. It is activated by ground commands and left on for specific durations when unusual or interesting activity is expected[8].

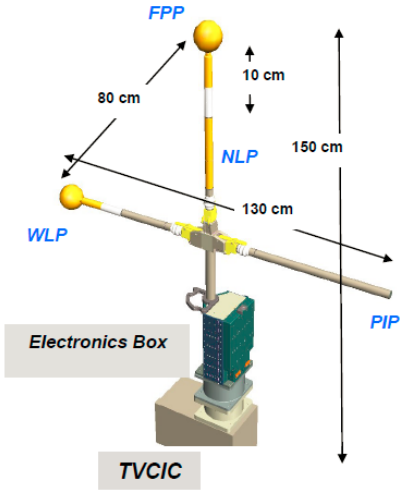

FPMU Instrument Characteristics

Sensor	Measured Parameter	Rate (Hz)	Effective Range
FPP	V_F	128	-180 V to +180 V
WLP	N T_e V_F	1	10^9 m^{-3} to 5x10^{12} m^{-3} 500 K to ~10,000 K -20 V to 80 V
NLP	N T_e V_F	1	10^9 m^{-3} to 5x10^{12} m^{-3} 500 K to ~10,000 K -180V to +180 V
PIP	N	1	1.1x10^{10} m^{-3} to 4x10^{12} m^{-3}

[*Wright et al.*, 2008; *Barjatya et al.*, 2009]

Figure 3 *- FPMU Specifications*

There are four individual probes that make up the FPMU, they are the Floating Potential Probe (FPP), Wide Sweep Langmuir Probe (WLP), Narrow Sweep Langmuir Probe (NLP), and Plasma Impedance Probe (PIP), shown in Figure 3. The left side of the figure gives the dimensions of the instrument while the table shown the ranges on the measurements that can be made; V is potential, N is ion density, and T is ion temperature.

FPP – The FPP is a 5.08 cm radius gold plated sphere on top of the FPMU which measures the potential of the surrounding plasma at 128 Hz relative to the ISS ground. It is separated electrically from the ISS chassis by a high impedance circuit on the order of 10^{11} ohms.

WLP – The WLP is a sphere identical to the FPP located on one of the branches of the FPMU. It sweeps between -20 V and 80 V relative to the ISS ground. The resulting current is measured at 1 Hz. From the sweeping measurements, the potential, ion density, ion temperature can be calculated.

NLP – The NLP is a gold plated cylinder of radius 1.43 cm and length 5.08 cm. It is additionally surrounded by guard cylinders of radius 1.43 cm and length 10.2 cm. Located on the shaft of the FPP, it sweeps between -4.9 V and 4.9 V with the current measured at 1 Hz. The NLP voltage is relative to the voltage being measured by the FPP, and so can act as a check on the FPP measurements. Similar to the WLP, the potential difference, ion density, and ion temperature can be calculated using the current measurements.

PIP – The PIP is a short dipole antenna located on the other branch of the FPMU and is electrically isolated from the ISS. It generates signals from 100 kHz to 20 MHz and measures the impedance (both magnitude and phase) of the surrounding plasma. The plasma density is found using this measurement.

Ionosphere

The ionosphere is the layer of the Earth's atmosphere in which the ISS orbits. It is a plasma made up of a high concentration of ions and free electrons. It starts at about 80 km above the Earth's surface and extends to about 1000 km. As shown in Figure 4, it is made up of several layers. The D and E layers disappear on the night side, while the F1 and F2 layers combine into a single F layer.

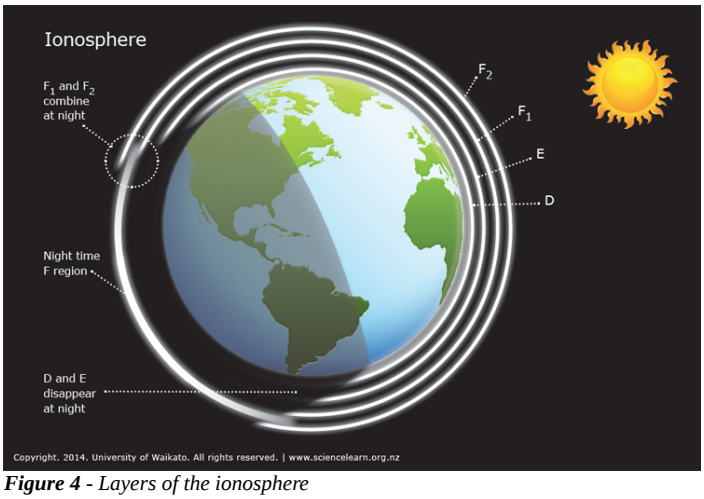

Figure 4 *- Layers of the ionosphere*

Geomagnetic Storms

Geomagnetic storms are caused by a shock or increase in the solar wind pressure, combined with a southward turning of the interplanetary magnetic field. Due to the Earth's magnetic field being coupled with the solar wind, this will compress the magnetic field and cause auroral currents to be disturbed. A storm is identified by the disturbance storm time index (Dst)[9] which indicates the strength of the ring currents around the Earth. A negative Dst shows the magnetic field generated by these currents has weakened the Earth's magnetic field.

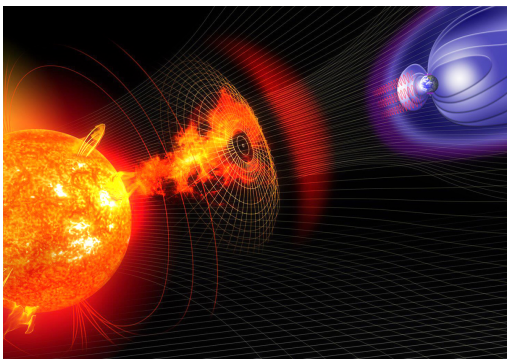

Figure 5 *- Depiction of a CME aimed at the Earth*

Of the intense storms seen by the Earth, about 85% of them are caused by coronal mass ejections (CME) and the other 15% are caused by co-rotating solar wind streams[10]. During the initial phase of a storm, the magnetic field of the Earth will increase due to the compression and the Dst will

increase as well. Not all storms will have an initial phase. The storm then progresses into the main phase, marked by a large decrease in the Dst. During this phase, strong ring currents can develop in the equatorial region of the Earth's magnetic field. The final phase is the recovery phase, where Dst levels return to normal, often within a couple of days.

Methodology

To start, I used data files found on Coordinated Data Analysis Web (CDAweb). These were computable document format (cdf) files containing the ion density and ion temperature measurements derived from the NLP. To read the cdf files and work with the data I used Interactive Data Language (IDL). I modified the program read_cdf_fpmu.pro to work with these cdf files. I made plots of the data using the tplot library for IDL. The plotting was done with plot_cdf_fpmu.pro. I began by matching previously published plots to confirm my analytical method.

In the density plot the values would occasionally jump by several orders of magnitude from one sample to the next and then return as seen in panel 1 of Figure 6. I imposed an upper limit and removed all values over the limit, setting them to not a number (NAN).

The temperature data would occasionally have data points that would drop to -9999, shown in Figure 6, panel 2. I filtered these by setting any point that was -9999 as NAN.

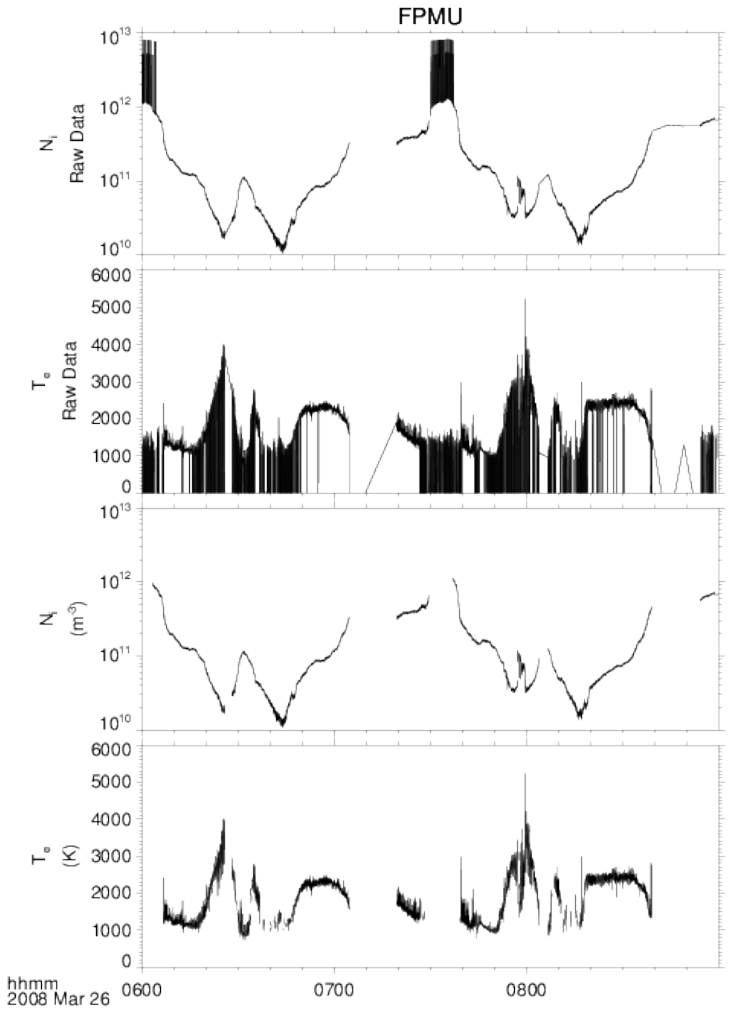

Figure 6 *- Data plots before data cleaning (Panel 1 and 2) and after cleaning (Panel 3 and 4)*

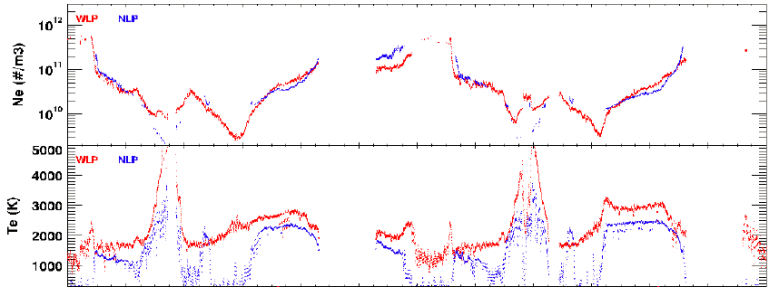

Figure 7 *- Published data plots of ion density and ion temperature*

Lastly, the plots would connect all adjacent points when plotting, even if there was a significant time gap between points. I fixed this by choosing a reference time interval and any interval larger than this had its two endpoints set as NAN so that the plot would not connect the points. The final results of the processing are shown in panels 3 and 4 of Figure 6. Figure 7 shows a published plot of the same data with density in panel 1 and temperature in panel 2. Panel 3 of Figure 6 matches the blue line in panel 1 of Figure 7. Panel 4 of Figure 6 likewise matches the blue line in panel 2 of Figure 7.

After the plots had been matched, I switched the coordinate system the data was in. The latitude and longitude given by the files were in geodetic coordinates. Geodetic coordinates have the z-axis going through the geographic poles and the x-axis going through the Prime Meridian. These coordinates rotate with the earth. An alternate coordinate system is the geomagnetic system. Figure 8 shows both coordinate systems, with geodetic on the left and geomagnetic on the right. Geomagnetic coordinates have the z-axis going through the two magnetic poles. The x-axis then points at the sun. This system also uses magnetic longitude, magnetic latitude (MLAT), and magnetic local time (MLT). Magnetic latitude and longitude are defined from the magnetic poles instead of the geographic poles with the longitudinal meridian as the connecting line closest to the sun. Rather than the grid being fixed on the Earth, the grid is fixed to the magnetic field and so does not move with the rotation of the Earth. Magnetic local time is a 24 hour system on this grid. The meridian is noon or MLT = 12 and the line opposite is midnight or MLT = 0. Since magnetic latitude and magnetic local time would be more practical for the investigation I wanted to do, I used an existing subroutine to perform the conversion from geodetic to geomagnetic.

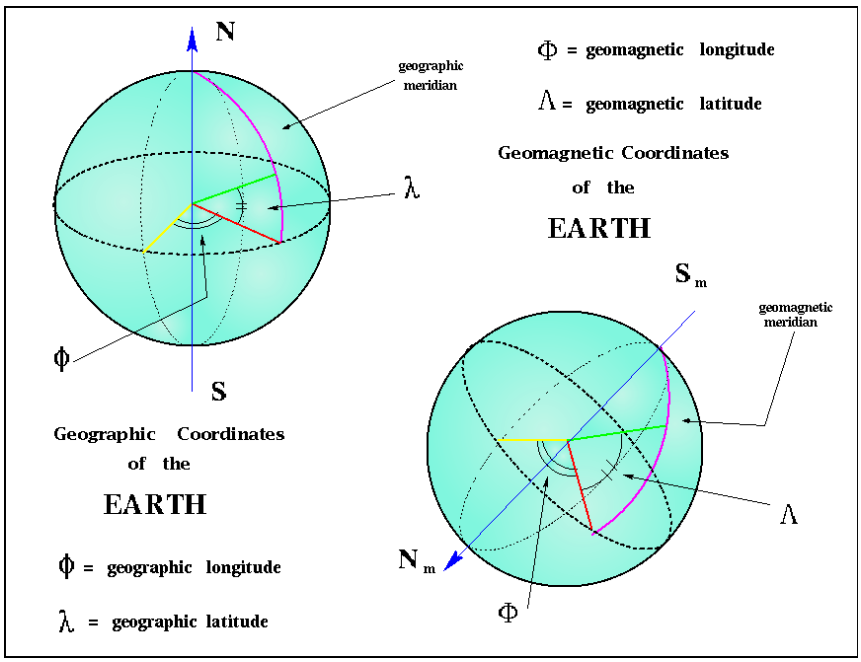

Figure 8 *- Comparison of geographic (geodetic) and geomagnetic coordinates*

Once the data was formatted, I began looking at the environment. The first step was to identify storms where the FPMU had collected data for the duration of the storm. I generated a list of all storms from 2006 to 2016 with a Dst of less than -50 nT and compared the dates to the data available. This narrowed the number of storms to choose from 130 to 26. I plotted the remaining storms and any storms where significant data gaps were present within the files were also rejected. This brought the

potential storm count to 19. I chose the one remaining intense storm of Dst < -100 to evaluate. Of the medium storms remaining I rejected the weakest storms, potentially overlapping storms, and storms missing data at the critical points. The critical points were the calm before the storm, the peak of the storm, early recovery, and late recovery. From the last 5 storms standing, I picked the one with the most complete data.

After the two storms were chosen, I plotted the entire duration of the storms in two hour intervals in order to look closely at the critical points. Any plot that was missing more than a third of this period was thrown out. To simplify the comparison, I also limited myself to plots where the two hour period contained one complete period of the ISS orbit. From these I picked plots that best showed the critical points of the storms.

Observations

The moderate storm chosen occurred on 09-20-2015 and had a minimum of -76.6 nT Dst. The intense storm occurred on 12-20-2015 and had a minimum of -171.5 nT Dst. Both storms were caused by CMEs. The overall storm Dst profiles are shown in Figure 9, with the September storm on the top and the December storm on the bottom.

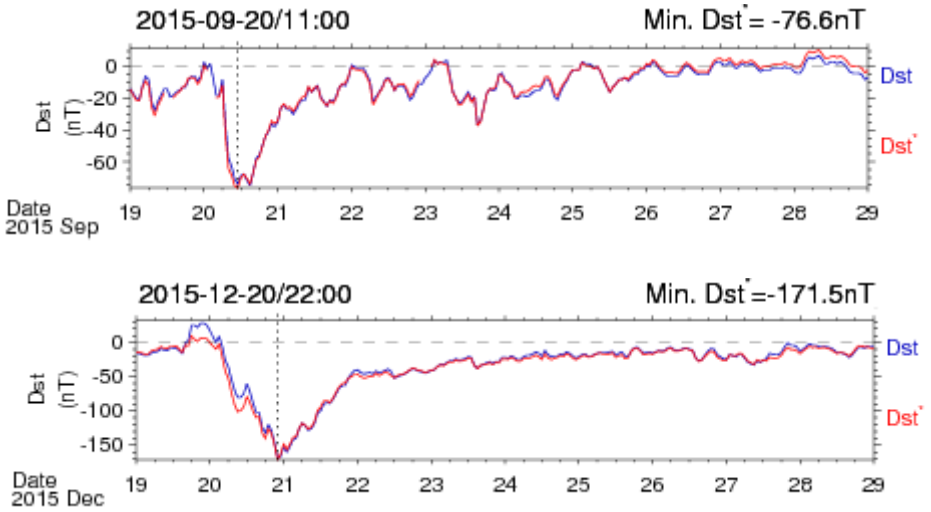

Figure 9 *- Dst profiles of the two storms chosen. The top is 2015-09-20 and the bottom is 2015-12-20*

Calm

I looked at the calm periods before the storms in order to establish what normal orbital conditions were. Figure 10 shows the calm periods of both storms, September on the left and December on the right. The panels of each storm from top to bottom show the ion density, ion temperature,

altitude, MLAT, MLT, and sunlight seen by the ISS. Ion density appeared to have an inverse relationship with altitude that can be seen when comparing panels 1 and 3 with lower altitudes caused the density to rise. There was also increased variation in both the density and temperature when the ISS was crossing the magnetic equator on the night side. The night side is shown by the sunlight plot (panel 6) when the % sunlight is equal to zero and the crossing is when the MLAT plot (panel 4) changes sign. The effect was more noticeable in the density plot than the temperature plot. The September storm also had a small depletion in the density just before the ISS crossed the line between sun and shadow, called the terminator. The terminator can be identified by the % sunlight plot when it goes from 0% to 100% (shadow to sun) or from 100% to 0% (sun to shadow).

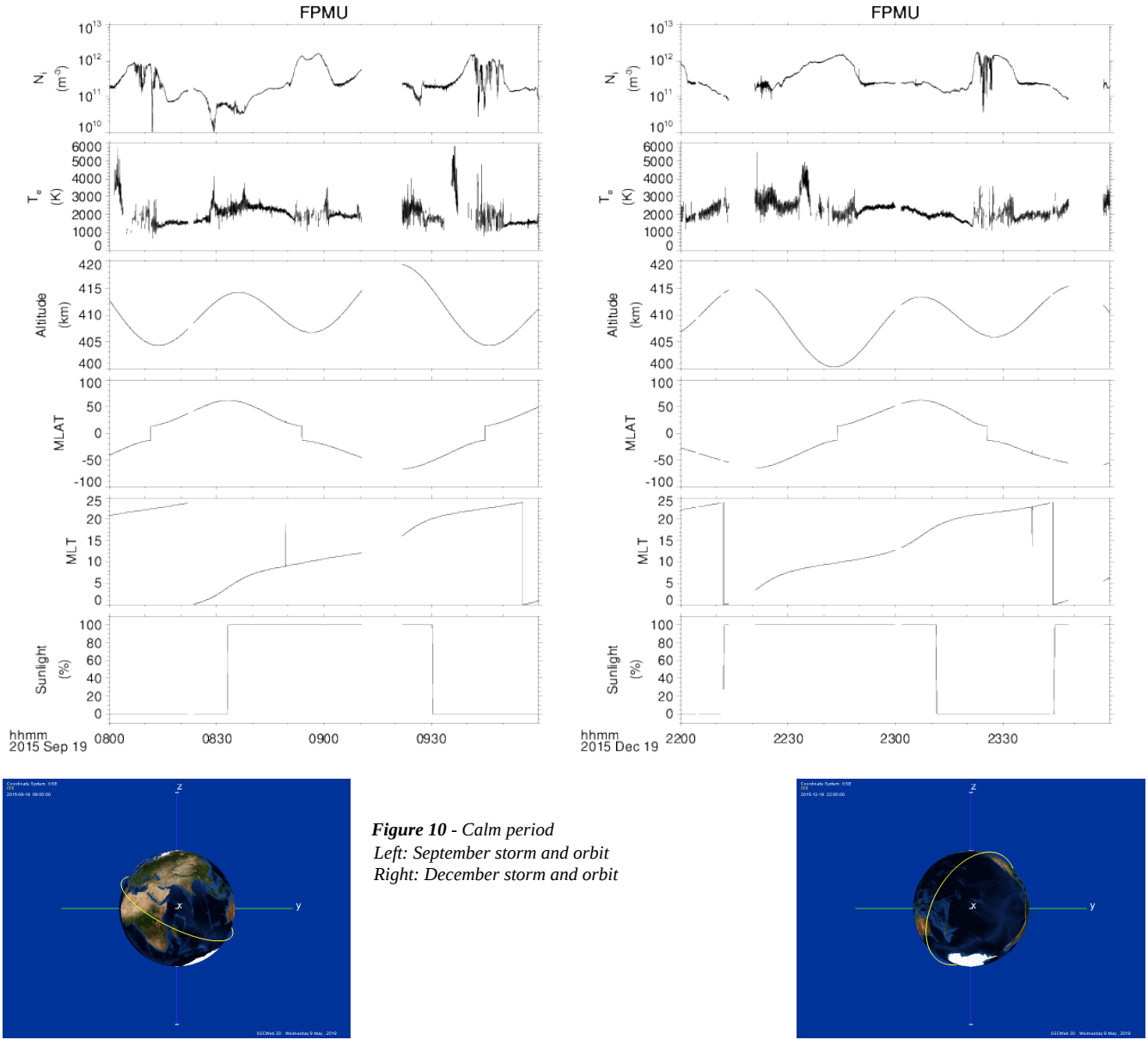

Figure 10 *- Calm period*
Left: September storm and orbit
Right: December storm and orbit

Peak

The peak of the storm, shown in Figure 11, occurred when the Dst reached a minimum. For both storms, the altitude dependence of density weakened. However, the most noticeable effect was that the variations in density and temperature from the night equatorial crossing completely disappeared for both storms. Lastly, while the depletions near the terminator remain in the September storm, one also appeared in the December storm when the ISS crossed from the shadow into the sunlight.

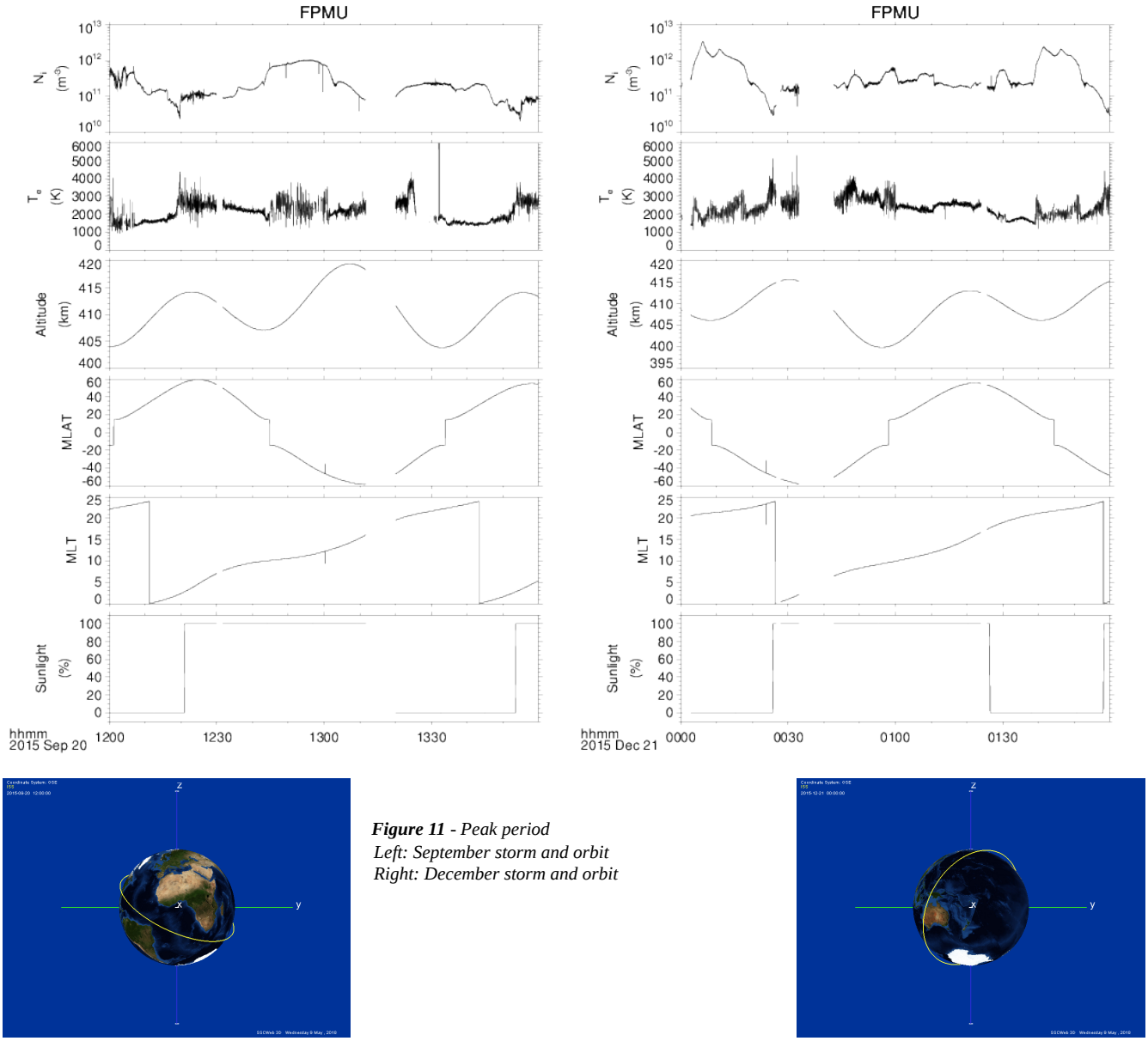

Figure 11 *- Peak period*
Left: September storm and orbit
Right: December storm and orbit

Early Recovery

Figure 12 shows the conditions approximately a day after the peak for both storms. The altitude dependence can be seen again in the density plot and the variations from the night equatorial crossings for both density and temperature have returned. However, all depletions seen at the terminators are now absent in both storms.

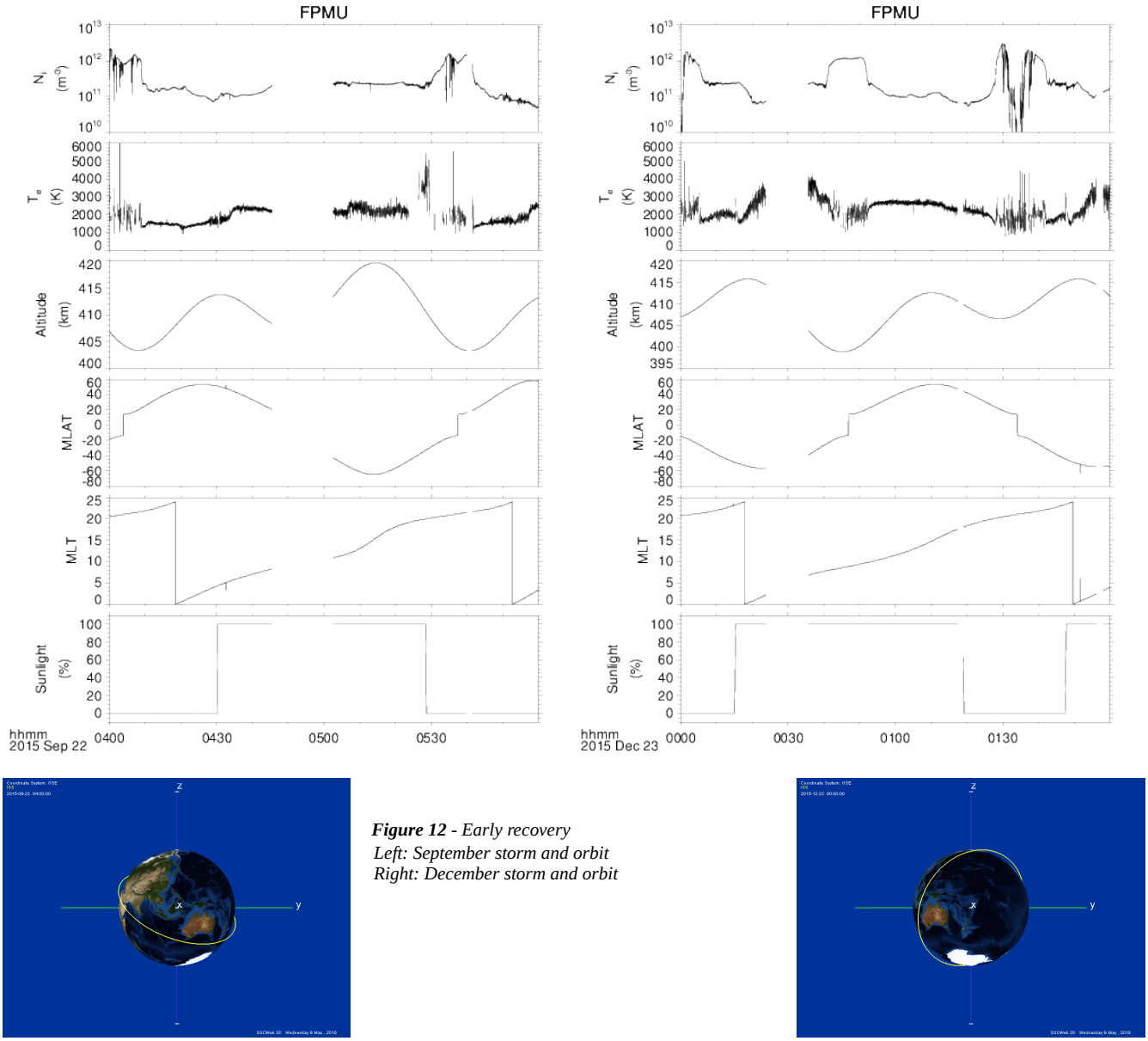

Figure 12 *- Early recovery*
Left: September storm and orbit
Right: December storm and orbit

Long Recovery

The only difference from the short term recovery for the September storm seems to be that the depletions may have returned. Figure 13 panel 1 shows a data gap roughly where the first depletion would be and while the second depletion appears to be there, it is close enough to the night equatorial crossing that it isn't clear if it is due to crossing the terminator or crossing the equator. For the December storm, it shows that the ISS is in 100% daylight at all times and so may not be a good comparison. There are no depletions or night crossing variations, but this would be expected as the ISS isn't crossing the terminator and so isn't performing a night crossing. Also, the altitude dependence of density appears to be weaker than expected at one point and stronger at the other. The bump seen in density more accurately corresponds to the equator crossing instead.

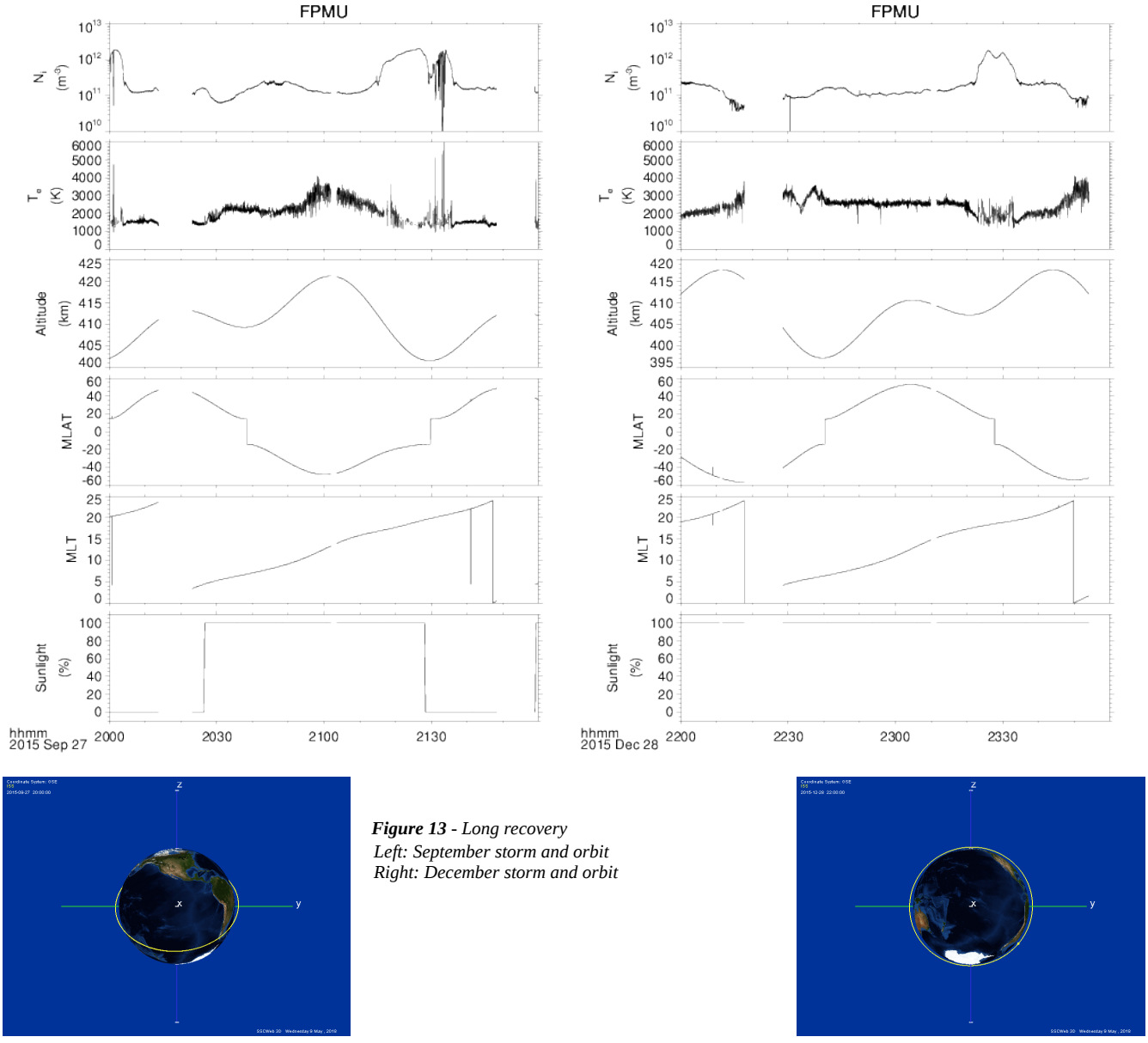

Figure 13 *- Long recovery*
Left: September storm and orbit
Right: December storm and orbit

Discussion

As seen from the observations, there are a great many changes that occur in the density and temperature around the ISS just from its orbit. Because of this, it is a little harder to isolate which changes were a result of the CMEs and which were normal.

The altitude dependence observed is a known effect as shown in Figure 14, which shows the average densities of the F Layer of the Ionosphere for the day and night side. However this may not explain all of the change since there were areas where this dependence weakened or disappeared. All of the low altitude periods also occurred at roughly the same time as equator crossings which makes it impossible to isolate from any effect the crossing might have had.

The equator crossings strongly influenced the environment around the ISS. This was shown in Figure 10 where there are clear variations at the night equatorial crossing. This is also be supported by Figure 13 where in the December storm the density seems more affected by the crossing rather than the altitude. It's also the feature that showed the most prominent change during the CME as shown in Figure 11 when the variations at the night crossing disappeared.

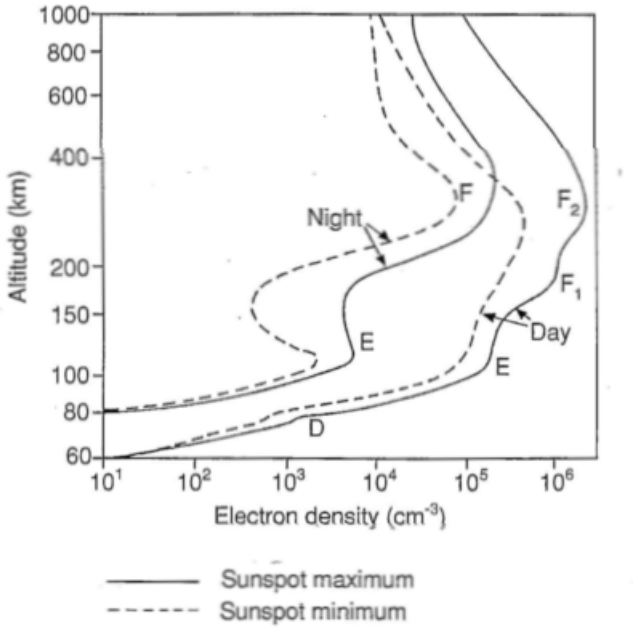

Figure 14 *- Known density dependence on altitude*

Finally, the depletions before the terminator crossings were more noticeable in the September storm than the December storm. They were also present during the peak of the storms but absent in both storms during recovery. The depletions may be caused by an effect that is strongest slightly after the peak of the storms and recovers later. Alternatively the differences between the storms could point to either a seasonal influence or an orbital path influence. In September the storm occurred close to the equinox and the ISS had a more equatorial orbit. In December the storm happened near solstice and the ISS had a more polar orbit.

Summary

A more thorough study of the data would need to isolate all of the normal seasonal and orbital conditions. After all of those factors had been identified, a more in depth look at the effects of geomagnetic storms could be done. Data from more storms as well as quiet periods would help

determine which effects are caused by storms and which are not. It would also help to look at the data taken by the other probes on the FPMU and compare with the NLP's data for the storm. The other probes may not have the same data gaps as the NLP or possibly may have observed features where the NLP missed them.

Acknowledgements

I would like to thank Jichun Zhang for acting as my primary advisor on this project and assisting me with data processing. I also want to thank Lynn Kistler for also assisting as an advisor. I would lastly like to thank Victoria Coffey for her advice and help with acquiring the data files from CDAweb.

References

[1] Wright, K. H. Jr., Swenson, C. M., Thompson, D. C., Barjatya, A., Koontz, S. L., Schneider, T. A., … Bui, T. H. (2008). Charging of the International Space Station as Observed by the Floating Potential Measurement Unit: Initial Results. *IEEE Transactions on Plasma Science, Vol. 36* (5), 2280-2293.

[2] Evans, C. A., Robinson, J. A., Tate-Brown, J., Thumm, T., Crespo-Richey, J., Baumann, D., Rhatigan, J. (2009). International Space Station Science Research Accomplishments During the Assembly Years: An Analysis of Results from 2000-2008. *NASA/TP-2009-213146-Revision A.*

[3] USURF. (2006, July 31). SDL Sensor to be Installed on International Space Station. *SDL – 2006 Press Releases*. Retrieved from http://www.sdl.usu.edu/

[4] USURF. (2003, October 14). The Space Dynamics Laboratory Completes Floating Potential Measurement Unit. *SDL – 2003 Press Releases*. Retrieved from http://www.sdl.usu.edu/

[5] Coffey, V. N., Wright, K. H. Jr., Minow, J. I., Schneider, T. A., Vaughn, J. A., Craven, P. D., … Bui, T. H. (2008). Validation of the Plasma Densities and Temperatures From the ISS Floating Potential Measurement Unit. *IEEE Transactions on Plasma Science, Vol. 36* (5), 2301-2308.

[6] Minow, J. I., Wright, K. H. Jr., Chandler, M. O., Coffey, V. N., Craven, P. D., Schneider, … Alred, J. W. Summary of 2006 to 2010 FPMU Measurements of International Space Station Frame Potential Variations.
(Power point presentation provided by Victoria Coffey)

[7] FPMU Floating Potential Measurement Unit Fact Sheet. *Space Dynamics Laboratory Utah State University Research Foundation*. Retrieved from http://www.spacedynamics.org/

[8] Barjatya, A., Swenson, C. M., Thompson, D. C., Wright, K. H. Jr. (2009). Invited Article: Data analysis of the Floating Potential Measurement Unit aboard the International Space Station. *Review of Scientific Instruments, Vol. 80*. 041301-1 – 041301-11.

[9] Gonzales, W. D., Joselyn, J. A., Kamide, Y., Kroehl, H. W., Rostoker, G., Tsurutani, B. T., Vasyliunas, V. M., (1994). What is a geomagnetic storm?. *Journal of Geophysical Research, Vol. 99* (A4), 5771-5792.

[10] Zhang, J., Richardson, I. G., Webb, D. F., Gopalswamy, N., Huttunen, E., Kasper, J. C., … Zhukov, A. N., (2007). Solar and interplanetary sources of major geomagnetic storms (Dst ≤-100 nT) during 1996-2005. *Journal of Geophysical Research, Vol. 112*. A10102-1 – A10102-19.

[11] Huang, C. (2008). Continuous penetration of the interplanetary electric field to the equatorial ionosphere over eight hours during intense geomagnetic storms. *Journal of Geophysical Research, Vol. 113*. A11305-1 – A11305-10.

[12] Coffey, V., Sazykin, S. Chandler, M. O., Hariston, M., Minow, J. I., Anderson, B. J. Observations of deep ionospheric F-region density depletions with FPMU instrumentations and their relationship with the global dynamics of the June 22-23, 2015 geomagnetic storm.
(Paper provided by Victoria Coffey)

[13] Vita, S. K., (2017). FPMU Data Analysis of Ionospheric Plasma Depletions. *NASA – Internship Final Report, Fall 2017 Session*.

[14] Irrgang, W. C. (2017). Correlating ISS Floating Potential Data with Geomagnetic Storms. *NASA – Internship Final Report, Summer 2017 Session*.

Figures

Figure 1 - https://spaceflight.nasa.gov/gallery/images/shuttle/sts-132/html/s132e012208.html

Figure 2 - [6]

Figure 3 - [6]

Figure 4 - https://www.sciencelearn.org.nz/images/248-layers-of-the-ionosphere

Figure 5 - http://www.freedompreppers.com/coronal-mass-ejection.htm

Figure 7 - [6]

Figure 8 - http://hpamsmi2.mi.infn.it/~wwwams/geo.html

Figure 14 - Hargreaves (1992)

All other figures produced by me